PHYSICAL REVIEW E **94**, 022422 (2016)

Partial synchronous output of a neuronal population under weak common noise: Analytical approaches to the correlation statistics

Alexandra Kruscha and Benjamin Lindner
Bernstein Center for Computational Neuroscience, Berlin, 10115, Germany
and Institute for Physics, Humboldt-Universität zu Berlin, Berlin, 12489, Germany
(Received 20 April 2016; published 29 August 2016)

We consider a homogeneous population of stochastic neurons that are driven by weak common noise (stimulus). To capture and analyze the joint firing events within the population, we introduce the partial synchronous output of the population. This is a time series defined by the events that at least a fixed fraction $\gamma \in [0,1]$ of the population fires simultaneously within a small time interval. For this partial synchronous output we develop two analytical approaches to the correlation statistics. In the Gaussian approach we represent the synchronous output as a nonlinear transformation of the summed population activity and approximate the latter by a Gaussian process. In the combinatorial approach the synchronous output is represented by products of box-filtered spike trains of the single neurons. In both approaches we use linear-response theory to derive approximations for statistical measures that hold true for weak common noise. In particular, we calculate the mean value and power spectrum of the synchronous output and the cross-spectrum between synchronous output and common noise. We apply our results to the leaky integrate-and-fire neuron model and compare them to numerical simulations. The combinatorial approach is shown to provide a more accurate description of the statistics for small populations, whereas the Gaussian approximation yields compact formulas that work well for a sufficiently large population size. In particular, in the Gaussian approximation all statistical measures reveal a symmetry in the synchrony threshold γ around the mean value of the population activity. Our results may contribute to a better understanding of the role of coincidence detection in neural signal processing.

DOI: 10.1103/PhysRevE.94.022422

I. INTRODUCTION

Synchronous neuronal activity is ubiquitous in the nervous system. In many neuronal systems, like in visual [1] or olfactory [2] sensory cells, experiments revealed that the synchronous activity of neuronal assemblies carries special information about sensory stimuli. It is therefore believed that precise temporal relations between the discharges of the neurons impact the ability of target neurons to represent sensory stimuli. The synchronous spiking of neuronal assemblies can be read out by post-synaptic neurons by means of coincidence detection. Reference [3] suggested that coincidence detection is a prevalent operation mode of cortical neurons.

A very simple form of temporal precision becomes manifest by joint firing of a sizable fraction of a group of neurons (population) within a small time window. Such synchronous events can occur by chance in completely independent neurons, they can arise due to recurrent connectivity, or they can be caused by common stimuli. Here, we focus on synchrony induced by common stimuli (due to overlapping receptive fields) rather than by coupling between the neurons. Populations of uncoupled neurons with overlapping receptive fields can be found, for instance, at the first stage of sensory input processing. Examples are auditory nerve cells [4], olfactory receptor neurons in insects [5,6], and electroreceptors in weakly electric fish [7]. Experimental studies on the effect of common noise can be found in Refs. [8–11]. In particular, the synchronizing effect induced by common noisy stimulation was experimentally investigated in [12–14].

In the past, different groups have developed analytical approximations for the statistics of pairs of neurons and of the summed activity of a population under common drive [10,15–21]. Although synchrony measures have been debated in the literature, the idea of a time-dependent synchronization variable, that potentially encodes specific information on the common stimulus, has received comparatively little attention [14,22].

Reference [22] investigated the information transmission between a common stimulus and the total synchronous firing of a neuronal population. In this theoretical study a rather strict measure of synchrony was used. A synchronous event was defined by the joint firing of *all* neurons within a short time window.

Here, we generalize the definition of the synchronous output, for which only a certain fraction γ of the population has to fire in synchrony, which should be in large populations a biologically more relevant scenario. It reflects the fact that a postsynaptic cell, having some firing threshold, needs a certain minimal number of action potentials to arrive within a short time.

In this paper, we focus on the effect of a weak common stimulus on the statistics of the partial synchronous output. Our paper is organized as follows. In the next section we introduce our model, different mathematical representations of the partial synchronous output, and the spike-train statistics of interest. We review previous analytical approaches in Sec. III. In Secs. IV, V, and VI we outline our approximations for the mean value, the cross-spectrum with the common stimulus, and the power spectrum of the synchronous output, respectively. In Sec. VII we inspect how the spectra depend on the temporal correlation structure of the stimulus. We summarize and discuss our results in Sec. VIII.

II. MODELS AND MEASURES

We consider a homogeneous population of N uncoupled spiking neurons, each of which having intrinsic,

independent Gaussian white noise sources $\xi_k(t), k \in \{1,\dots,N\}$ with $\langle \xi_k(t)\xi_{k'}(t')\rangle = \delta_{k,k'}\delta(t-t')$. Homogeneous means, that every neuron is given by the same stochastic dynamical system receiving identical mean input and therefore exhibiting the same average firing rate r_0. In addition, every neuron is stimulated by the same zero-mean Gaussian white noise process $s(t)$ with auto-correlation function $\langle s(t)s(t')\rangle = 2cD\delta(t-t')$, which we will refer to as the *common stimulus*. The intensity of $s(t)$ is therefore given by cD, D being the total noise intensity each neuron is subject to (intrinsic plus common noise) and $c \in [0,1]$ is the correlation coefficient of the input, which quantifies the identical fraction of the total noise each neuron receives. The parameter c determines how large the common external stimulus is in comparison to the independent intrinsic fluctuations. For $c = 0$ (no common stimulus), all neurons are completely independent. For $c = 1$, the independent fluctuations vanish such that every neuron in the population receives exactly the same input and thus behaves asymptotically (in the long-time limit) exactly the same way. Here, we focus on the case of a weak common stimulus, being small in comparison to the other inputs of the neuron ($c \ll 1$).

The theory we present is general and does not assume a specific spiking neuron model. To compare our analytical results to numerical simulations we apply our theory to a population of leaky integrate-and-fire (LIF) neurons, given by the single neuron voltage dynamics

$$\dot{v}_k = -v_k + \mu + s(t) + \sqrt{(1-c)2D}\xi_k(t), \tag{1}$$

where μ is the constant base current. Whenever the voltage v_k exceeds the threshold one, a spike is recorded and v_k is reset to zero. The corresponding spike trains are $x_k(t) = \sum_i \delta(t - t_{k,i})$, where the $t_{k,i}$ are the spike times of the kth neuron. The average firing rate r_0 of each neuron is the mean value of the spike train $r_0 = \langle x_k \rangle_{\xi_k,s}$. All necessary statistics for the LIF model are stated in Appendix A.

A. Partial synchronous output

We define for a population of N neurons the *partial synchronous output* $Y_\gamma(t)$ with *synchrony threshold* $\gamma \in \{0,1/N,2/N,\dots,1\}$ in the following way:

$$Y_\gamma(t) := \begin{cases} 1, & \text{if at least } \gamma N \text{ neurons} \\ & \text{spike within} [t-\Delta, t] \\ 0, & \text{else} \end{cases}. \tag{2}$$

The partial synchronous output is a two-state process and can be interpreted as a coarse representation of a postsynaptic cell which is activated (having the value one) if at least γN out of N presynaptic neurons fired together in a time window of width Δ (see Fig. 1 for illustration). In order for this postsynaptic cell to act as a coincidence detector, the bin width Δ (corresponding to the time over which a postsynaptic neuron integrates incoming input) has to be small in comparison to the inverse firing rate $1/r_0$ of the presynaptic neurons. We therefore demand that the product $R_0 := r_0\Delta$ is sufficiently small. Note that the definition, Eq. (2), can be applied to the output of model neurons or to that of real neurons alike. A simple way to study experimentally the synchronous response of uncoupled neurons to common noise is to use Eq. (2) for a set of trials, in which the same neuron is driven by the same frozen-noise stimulus. For the special case of $\gamma = 1$ and $N = 2$ this yields very similar results for the spectral statistics considered in this paper compared to the scenario in which distinct neurons are driven by the same stimulus [14].

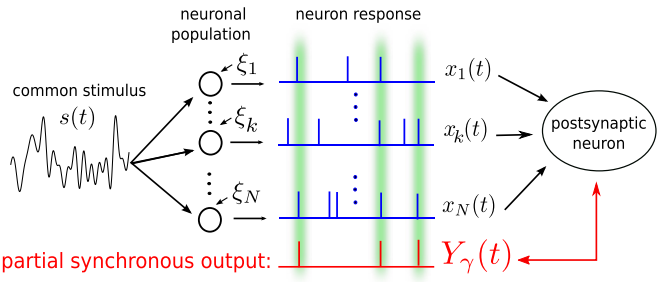

FIG. 1. Schematic representation of the model. A homogeneous population of N uncoupled neurons is subject to a common stimulus $s(t)$ and independent noise sources $\xi_k(t)$, leading to variable single neuron output spike trains $x_k(t)$. The partial synchronous output $Y_\gamma(t)$ measures the times where at least a fixed fraction γ of the population is active (shaded stripes). $Y_\gamma(t)$ can be interpreted as a coarse approximation of the activity of a postsynaptic neuron.

The naming 'synchronous output' might be misleading in some cases, for instance for $\gamma = R_0$. Note that R_0 is the average fraction of the population which is active within a time window of width Δ. This means that even if the neurons are completely independent of each other, on average $R_0 N$ of them fire simultaneously. Hence, only for synchrony thresholds γ that are sufficiently larger than R_0 does the process $Y_\gamma(t)$ truly measure (above-average) joint firing events.

We now introduce two distinct but completely equivalent ways of representing Y_γ in mathematical terms. To do so, we first convolve each spike train of the population with the boxcar function $\mathcal{B}(t) = \theta(t) - \theta(t-\Delta)$ (here $\theta(t)$ is the Heaviside function):

$$b_k(t) := \mathcal{B} * x_k(t) = \int_{t-\Delta}^{t} x_k(t')dt', \tag{3}$$

where the asterisk stands for the convolution $g_1 * g_2(t) = \int_{-\infty}^{\infty} g_1(t')g_2(t-t')dt'$. The function $b_k(t)$ can be seen as a *box train* where each spike of x_k at time t_i is substituted by a box of hight one going from t_i to $t_i + \Delta$ (see Fig. 2 upper row). All these box trains are statistically equivalent. In the following, an arbitrary representative of these processes $b_k(t), k \in \{1,\dots,N\}$, will be referred to by $b(t)$ (without an index).

The *population activity* A is then the sum of these box trains, divided by the population size

$$A = \frac{1}{N}\sum_{k=1}^{N} b_k. \tag{4}$$

The population activity $A(t)$ is a dimensionless discrete variable, $A \in \{0,1/N,2/N,\dots,1\}$. It states the fraction of the population that has been active within $[t-\Delta,t]$, i.e., it is the normalized spike count and differs from the standard definition of a rate [23]. If $A(t) = 0$, then there was no spike within $[t-\Delta,t]$, whereas $A(t) = 1$ corresponds to the case where all neurons fired simultaneously (assuming a sufficiently small

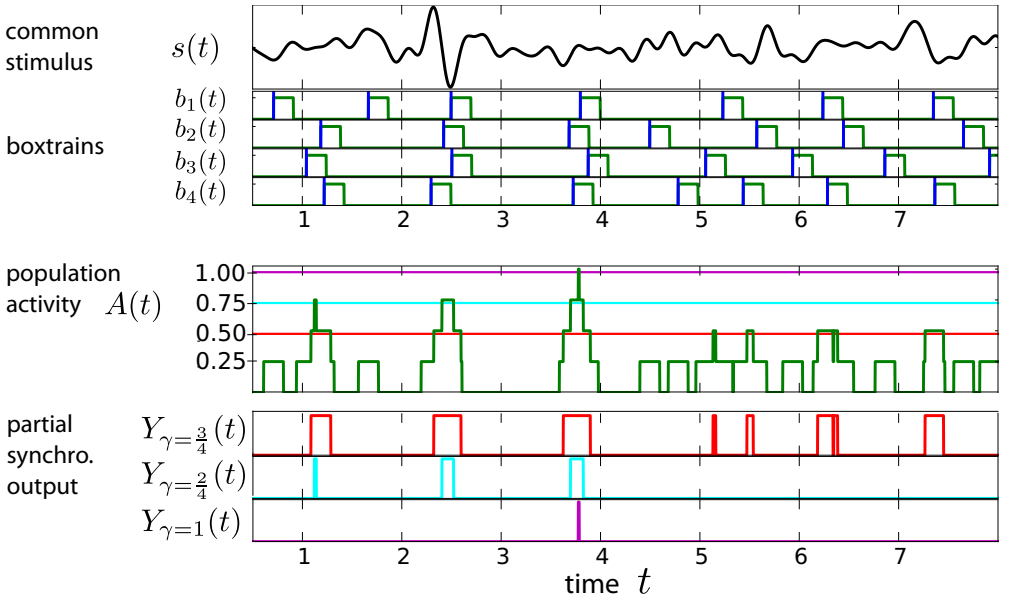

FIG. 2. Illustration of the measurement of the synchronous output $Y_\gamma(t)$, given by Eq. (5), for different synchrony thresholds γ for a population of $N = 4$ neurons. Top: Each spike train of the population is convolved with a box of hight one and width Δ. The population activity $A(t)$ (middle row) is the sum of these 'box trains' divided by the population size. The partial synchronous output (bottom rows) is one whenever the population activity is larger or equal to γ and zero otherwise.

bin width Δ, such that the probability that a single neuron fires twice in one bin can be neglected). A synchronous event with synchrony threshold γ is then simply given if the population activity is larger or equal to γ, such that the partial synchronous output can be written as

$$Y_\gamma = \theta\left(A - \gamma + \frac{1}{2N}\right), \tag{5}$$

where $\theta(t)$ is again the Heaviside step function. Figure 2 illustrates this activity-based representation of the synchronous output for a population of four neurons.

1. *Combinatorial representation of the synchronous output*

The Heaviside function in Eq. (5) makes a direct analytical calculation of important statistics of Y_γ difficult. We can, however, avoid the Heaviside function by generalizing an ansatz introduced in [22]. Not only the sum of the box-trains, but also their products contain information about the population's synchrony. If there are, for example, exactly n neurons (let us say the first n neurons of the population) that fired within $[t-\Delta, t]$, then the product of their box trains, $\prod_{k=1}^{n} b_k = b_1 \cdot b_2 \cdot \ldots \cdot b_n$, is one at time t, whereas all higher order products are zero. Hence, in order to check if at least γN neurons fired, one must look at all combinations of products of γN neurons:

$$\kappa = \sum_{\substack{\text{over all}\binom{N}{\gamma N}\\ \text{combinations } \pi}} \prod_{k=1}^{\gamma N} b_{\pi_k}, \tag{6}$$

$\kappa(t)$ is non-zero if at least γN neurons fired within $[t-\Delta, t]$. However if more fired, let us say n, then $\kappa = \binom{n}{\gamma N}$, because there are $\binom{n}{\gamma N}$ combinations that contribute with a one in Eq. (6). In order to derive again a two-state process for the synchronous output, one must take into account all higher order products:

$$Y_\gamma = \sum_{j=\gamma N}^{N} a_j \sum_{\substack{\text{over all}\binom{N}{j}\\ \text{combinations } \pi}} \prod_{k=1}^{j} b_{\pi_k} \tag{7}$$

with the combinatorial factor

$$a_j = (-1)^{j-\gamma N}\binom{j-1}{j-\gamma N}. \tag{8}$$

This representation of the partial synchronous output, which we will refer to as *the combinatorial approach*, does indeed coincide with the activity-based representation Eq. (5). The derivation of the prefactors a_j is given in Appendix B.

B. Statistics of interest

Our aim is to derive statistical properties of the synchronous output, namely its average value $\langle Y_\gamma \rangle$, its power spectrum and its cross-spectrum with the common signal. In numerical simulations we calculate the power spectrum of X and the cross-spectrum between two stationary stochastic processes $X(t)$ and $Z(t)$ by

$$S_X(f) = \lim_{T\to\infty} \frac{\langle \tilde{X}_T(f)\tilde{X}_T^*(f)\rangle}{T} \quad \text{and}$$
$$S_{X,Z}(f) = \lim_{T\to\infty} \frac{\langle \tilde{X}_T(f)\tilde{Z}_T^*(f)\rangle}{T}, \tag{9}$$

where the brackets $\langle\rangle$ denote averaging over repeated trials. The asterisk stands for the complex conjugate and $\tilde{X}_T$ is finite-time-window Fourier transform

$$\tilde{X}_T(f) = \int_{-T/2}^{T/2} dt\ X(t) e^{i2\pi f t}$$

with T being the size of the measurement time window which is centered around $t = 0$.

In the analytical calculations we make use of the Wiener-Khinchin-Theorem and derive the cross-spectrum via the Fourier transform of the cross-covariance $C_{XZ}(\tau) := \langle X(0)Z(\tau)\rangle - \langle X\rangle\langle Z\rangle$ and the power spectrum by the Fourier transform of the autocovariance $C_{XX}(\tau)$,

$$S_{X,Z} = \tilde{C}_{ZX}, \tag{10}$$

$$S_X = \tilde{C}_{XX}. \tag{11}$$

The tilde indicates the formal Fourier transform

$$\tilde{C}(f) = \int_{-\infty}^{\infty} dt\ C(t)e^{i2\pi ft}. \tag{12}$$

Note that we define the spectra without the DC-peak.

III. PREVIOUS ANALYTICAL APPROACHES AND RESULTS

A. Linear response ansatz

For weak stimuli $s(t)$, the instantaneous firing rate of the single neuron can be approximated by the linear response relation [24–26]

$$r(t) = \langle x_k\rangle_{\xi_k}(t) = r_0 + K * s(t), \tag{13}$$

where $K(t)$ is the linear response function and r_0 is the mean firing rate. This ansatz leads for the single box train, $b_k = \mathcal{B} * x_k$, to

$$\begin{aligned} R(t) :&= \langle b_k\rangle_{\xi_k}(t) = \int_{t-\Delta}^{t} r(t')dt' \\ &= r_0\Delta + \mathcal{B} * K * s(t) \\ &=: R_0 + s_e(t), \end{aligned} \tag{14}$$

where we used in the first line that $\langle \mathcal{B} * x_k\rangle = \mathcal{B} * \langle x_k\rangle$, since the convolution with $\mathcal{B}$ is a linear operation. The windowed firing rate $R(t)$ is the probability that a neuron spikes within $[t-\Delta, t]$, conditioned on a fixed realization of the common stimulus up to time t. On average, a neuron spikes with probability $R_0 = r_0\Delta$ within this time window. For small stimuli this firing probability is modulated by the time dependent *effective stimulus*

$$s_e(t) := \mathcal{B} * K * s(t). \tag{15}$$

By the convolution theorem, its Fourier transform is given by

$$\tilde{s}_e(f) = \tilde{\mathcal{B}}(f)\chi(f)\tilde{s}(f), \tag{16}$$

where $\chi = \tilde{K}$ is the susceptibility of the firing rate of a neuron, driven by the current $\mu + \sqrt{2D}\xi(t)$. The stochastic process s_e is a linear functional of the Gaussian process s and therefore Gaussian as well. Like s, the effective stimulus is centered around zero, i.e., $\langle s_e\rangle = 0$, and its power spectrum is by Eqs. (9) and (16) given by

$$S_{s_e}(f) = |\tilde{\mathcal{B}}(f)\chi(f)|^2 S_s(f). \tag{17}$$

Here, $S_s(f) = 2cD$ is the power spectrum of the common white noise. The variance of the effective stimulus reads

$$\langle s_e^2\rangle = \int_{-\infty}^{\infty} S_{s_e}(f)df \tag{18}$$

$$= \Delta^2 \int_{-\infty}^{\infty} \mathrm{sinc}^2(\Delta\pi f)|\chi(f)|^2 S_s(f)df, \tag{19}$$

where the sinc function, $\mathrm{sinc}(x) = \sin(x)/x$, emerges from the Fourier transform of the box filter

$$|\tilde{\mathcal{B}}(f)| = \Delta\mathrm{sinc}(\Delta\pi f). \tag{20}$$

Within this linear response approach the power spectrum of the single box train reads

$$S_b(f) = |\tilde{\mathcal{B}}(f)|^2 S_x(f), \tag{21}$$

where S_x is the power spectrum of a single spike train [e.g., for an LIF-neuron S_x is given by Eq. (A4)]. The power spectrum of the population activity is according to Eq. (4) given by

$$S_A = \frac{1}{N}S_b + \left(1 - \frac{1}{N}\right)S_{b_k,b_{k'}}. \tag{22}$$

Using the linear response ansatz Eq. (14), the cross-spectrum between two different box trains equals the power of the effective stimulus [17–19]

$$S_{b_k,b_{k'}}(f) = S_{s_e}(f) \tag{23}$$

and thus we obtain for the activity's power spectrum

$$S_A = \frac{1}{N}S_b + \left(1 - \frac{1}{N}\right)S_{s_e}. \tag{24}$$

B. Large population limit—Gaussian approximation of activity

The population activity is a sum of identically distributed stochastic processes b_k. Having the central limit theorem in mind it is therefore plausible for large population sizes N to approximate A by a continuous Gaussian stochastic process. The obvious constraint that impedes a rigorous application of the central limit theorem is the non-zero global correlation between the box trains due to the common stimulus. However, because we only consider weak correlations, a normal distribution of the activity is shown to be a reasonable approximation of the true activity density distribution p_A for large values of N [21]:

$$p_A(A) \approx p_A^G(A) = \frac{1}{\sqrt{2\pi\sigma_A^2}}\exp\left[\frac{-(A-R_0)^2}{2\sigma_A^2}\right] \tag{25}$$

with mean activity $\langle A\rangle = R_0 = r_0\Delta$ and variance

$$\sigma_A^2 = \langle s_e^2\rangle + \frac{R_0 - R_0^2}{N}. \tag{26}$$

Note that even in the limit of an infinite population, the activity still displays variability, which is solely due to the common stimulus. Whenever we use this Gaussian approximation of the population activity, we indicate it by the suffix 'G'.

IV. MEAN PARTIAL SYNCHRONOUS OUTPUT

How often does a synchronous event occur and how does this depend on the synchrony threshold? This can be addressed by looking at the mean value of the partial synchronous output.

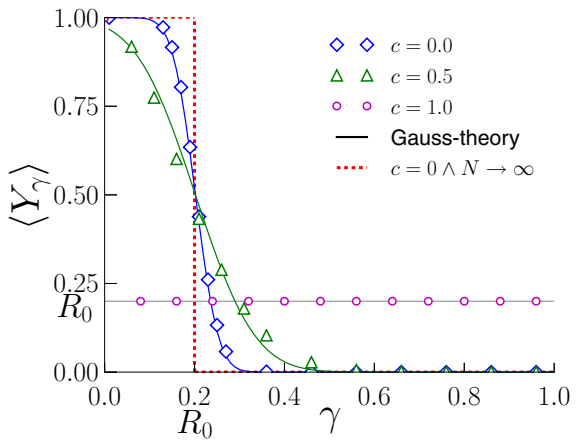

FIG. 3. Mean synchronous output vs synchrony threshold for different strength of the common noise as indicated. Symbols mark simulation results. The solid lines show the Gaussian approximation Eq. (30) for the cases $c \in \{0,0.5\}$. For an infinite large population and without any correlation ($c = 0$) (red dashed line), the mean synchronous output is either one for $\gamma \leqslant R_0$ or zero for $\gamma > R_0$. For full correlation ($c = 1$) (purple circles) the mean synchronous output equals the mean activity $R_0 = r_0\Delta$ for any $\gamma > 0$ (and is one for $\gamma = 0$). LIF-parameters: $\mu = 1.2, D = 0.01; \to r_0 = 0.58, N = 100, R_0 = 0.2$ (corresponding to the box width $\Delta = 0.35$).

If we use the activity-based definition, Eq. (5), the mean value of the synchronous output reads

$$\langle Y_\gamma \rangle = \left\langle \theta\left(A - \gamma + \frac{1}{2N} \right) \right\rangle, \tag{27}$$

where $\langle\rangle$ denotes the average over all independent noise sources $\xi = \{\xi_1, \xi_2, \ldots, \xi_N\}$ and the stochastic common signal s. Equation (27) is in a simple way related to the cumulative probability of the population activity

$$\langle Y_\gamma \rangle = \mathbb{P}(A \geqslant \gamma). \tag{28}$$

Hence, the mean synchronous output is simply the probability that the activity is equal to or above γ. Because $\mathbb{P}(A \geqslant \gamma) = \mathbb{P}(Y_\gamma = 1)$, the mean value $\langle Y_\gamma \rangle$ is the probability of having a partial synchronous event.

To give an overview over the possible limit cases, Fig. 3 shows how the mean synchronous output depends on the input correlation for the full range of $c \in [0,1]$. If the driving noise is identical for all neurons ($c = 1$), they all act asymptotically as one neuron, such that the activity can only have one of the two values, zero or one, and the probability for $A = 1$ is equal to R_0. Consequently, the mean value of the synchronous output is R_0 for any $\gamma > 0$ (see circles in Fig. 3). The other extreme is the case where all neurons are completely independent of each other ($c = 0$). For the limit of an infinitely large population the activity averages out the independent noise, such that for $c = 0$ the activity has the fixed value $A = \langle b \rangle = R_0$. The probability of having a synchronous output is therefore either one for $\gamma \leqslant R_0$ or zero for $\gamma > R_0$ (see red dashed line). For a finite population this step function is smoothed, resulting in a sigmoid function (see blue diamonds), because the activity can take different values around R_0. As c is increased, $\langle Y_\gamma \rangle$ undergoes a transformation from this sigmoid to the constant case for $c = 1$. We now show how $\langle Y_\gamma \rangle$ can be calculated for small input correlations c.

A. Gaussian approach

If we use the Gaussian approximation of the probability density of the population activity, Eq. (25), we can approximate Eq. (27) by

$$\langle Y_\gamma \rangle^G = \int_{\gamma - \frac{1}{2N}}^{\infty} p_A^G(A) \mathrm{d}A, \tag{29}$$

leading to the complementary error function

$$\langle Y_\gamma \rangle^G = \frac{1}{2} \mathrm{erfc}\left(\frac{\gamma - R_0 - 1/(2N)}{\sqrt{2}\sigma_A} \right). \tag{30}$$

For increasing population size the mean synchronous output approaches

$$\lim_{N\to\infty} \langle Y_\gamma \rangle^G = \frac{1}{2} \mathrm{erfc}\left(\frac{\gamma - R_0}{\sqrt{2\langle s_e^2 \rangle}} \right). \tag{31}$$

B. Combinatorial approach

If we use the combinatorial product representation of Y_γ, Eq. (7), we can directly compute the average of the synchronous output:

$$\langle Y_\gamma \rangle = \sum_{j=\gamma N}^{N} a_j \sum_{\substack{\text{over all} \binom{N}{j} \\ \text{combinations } \pi}} \left\langle \left\langle \prod_{k=1}^{j} b_{\pi_k} \right\rangle_\xi \right\rangle_s \tag{32}$$

$$= \sum_{j=\gamma N}^{N} a_j \binom{N}{j} \langle (R_0 + s_e)^j \rangle_s, \tag{33}$$

where we used that the intrinsic noise sources ξ_k of different neurons are independent of each other and we applied the linear response ansatz, Eq. (14). By the binomial theorem we can further evaluate

$$\langle (R_0 + s_e)^j \rangle_s = \sum_{k=0}^{j} \binom{j}{k} R_0^{j-k} \langle s_e^k \rangle. \tag{34}$$

Considering only orders up to the variance of the effective stimulus, we get the following combinatorial approximation of the mean synchronous output:

$$\langle Y_\gamma \rangle = \sum_{j=\gamma N}^{N} a_j \binom{N}{j} R_0^j \left[1 + \frac{j(j-1)}{2} \frac{\langle s_e^2 \rangle}{R_0^2} \right]. \tag{35}$$

In Fig. 4 both approximations of $\langle Y_\gamma \rangle$ are compared to numerical simulations of LIF populations for a weak common stimulus ($c = 0.1$). Figure 4(a) shows the mean for comparatively small populations, while in Fig. 4(b) the large population limit is explored. As can be seen in Fig. 4(a) the combinatorial approximation, Eq. (35), (dashed lines) is in excellent agreement with the numerical simulations (symbols). One limitation of its applicability, however, is the numerically expensive evaluation of the combinatorial factors in Eq. (35), which becomes intractable for large values of N. For this reason we apply the combinatorial approach only to small

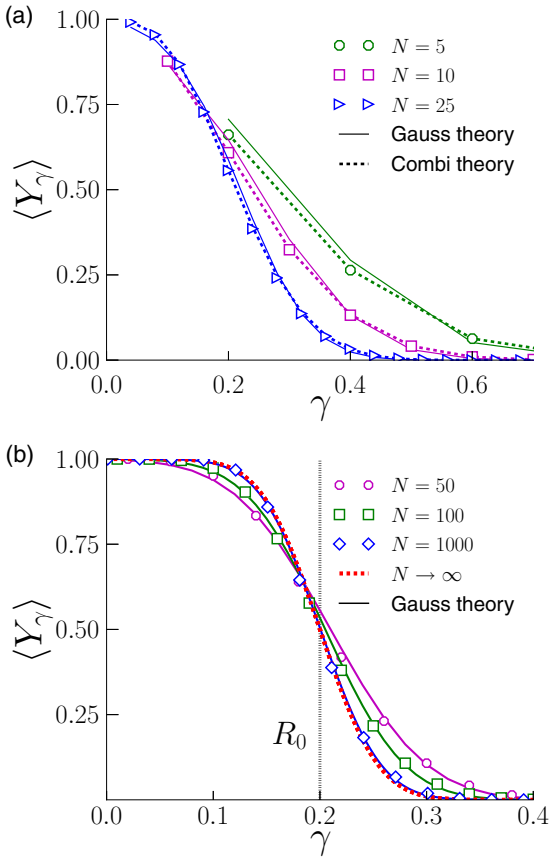

FIG. 4. The probability for a synchronous event is a sigmoid function of the synchrony threshold. Mean partial synchronous output $\langle Y_\gamma \rangle = \mathbb{P}(Y_\gamma = 1)$ versus synchrony threshold γ for LIF populations of various sizes N. (a) For small populations, simulation results (symbols) are compared to the Gaussian approximation, Eq. (30), (solid lines) and to the combinatorial theory, Eq. (35), (dashed lines). (b) For large populations simulations are compared to the Gaussian theory only. The red dashed line in b marks the limit case for an infinite large population given by Eq. (31). The vertical line marks the mean population activity R_0. Parameters: $\mu = 1.2, D = 0.01, c = 0.1, R_0 = 0.2$.

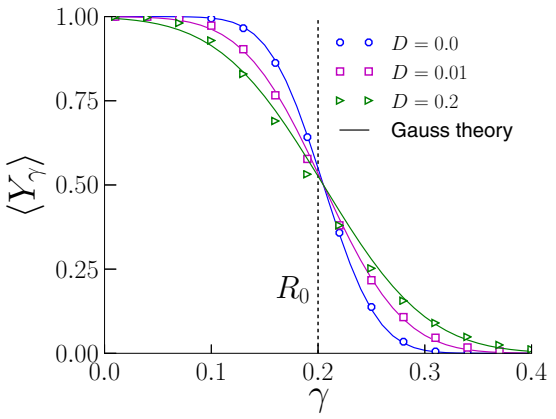

FIG. 5. Mean synchronous output for fixed input correlation $c = 0.1$ and for different total noise intensities $D \in \{0, 0.01, 0.2\}$ leading to the mean firing rates $r_0 \in \{0.56, 0.58, 0.80\}$. Simulation results (symbols) are compared to the Gaussian approximation, Eq. (30) (solid lines). Remaining parameters: $\mu = 1.2, R_0 = 0.2, N = 100$.

or moderately sized populations ($N < 50$). The Gaussian approach, Eq. (30), gives a reasonable approximation of the mean synchronous output (see solid lines), even though we consider only small populations in Fig. 4(a). In Fig. 4(b) we see that for large population sizes, the Gaussian approximation gives an adequate description of $\langle Y_\gamma \rangle$.

The probability of having a synchronous event is a sigmoid function of the synchrony threshold γ, if the input correlation is small. If γ is set notably below the mean population activity R_0, then the probability that the activity is above γ is close to one. In this case the population fires quasi always 'in synchrony'. In the other extreme, when γ is set exceedingly above R_0, i.e., when we demand a very large fraction of the population to fire simultaneously, the probability that the activity exceeds the value γ is close to zero. In this scenario there is hardly ever a synchronous event. Both extremes are therefore unfavorable to encode a weak time-dependent signal. The common signal is encoded in the change of the instantaneous population activity $A(t)$. In fact, for large populations, the activity is approximately given by $A(t) = \langle b \rangle_\xi = R_0 + s_e(t)$ [see Eq. (14)]. If γ is set too far away from the mean activity R_0, then this small change of A will not influence the synchronous output, which will be almost always one for $\gamma \ll R_0$ or almost always zero for $\gamma \gg R_0$. Hence, we can expect that the cross-correlation between the synchronous output Y_γ and the common signal s is maximal for $\gamma = R_0$.

Figure 5 shows the mean synchronous output for different values of the total noise intensity D for a fixed input correlation $c = 0.1$. An increase in the total noise results in an increase of the variance of the stimulus and with it to a larger value of the variance σ_A^2 [see Eq. (26)]. As a consequence, the integral over the distribution p_A, Eq. (29), i.e., $\langle Y_\gamma \rangle$, displays a slower decay in γ. Also for the deterministic case ($D = 0$), $\langle Y_\gamma \rangle$ is a sigmoid function if we assume an asynchronous initial state (random initial voltage values of the single neurons), resulting in a normally distributed activity. The Gaussian approximation, Eq. (30), works best for weak total noise, i.e., for small values of D.

V. CROSS-SPECTRUM BETWEEN COMMON NOISE AND PARTIAL SYNCHRONOUS OUTPUT

An important statistics that tells us how much the synchronous output is affected by the common stimulus, is their cross-spectrum. In the following we outline how the cross-spectrum can be approximated analytically and we test our approximations by comparison with numerical simulations.

A. Gaussian approach

If we approximate the population activity by a Gaussian process, we can apply the Bussgang theorem [27]. It states that for any two stationary Gaussian processes, the cross-correlation function taken after one of them has undergone a nonlinear transformation is identical to the cross-correlation of the two original signals up to a constant. In particular, let X and Z be stationary Gaussian processes with $\langle Z \rangle =$

0 and variances σ_X^2 and σ_Z^2, having the cross-covariance $C_{XZ}(\tau) = \langle X(0)Z(\tau)\rangle$. Then, for any transformation V, the cross-covariance between the distorted process $V(X)$ and the original signal Z is given by

$$C_{V(X)Z}(\tau) = \alpha C_{XZ}(\tau) \tag{36}$$

with the proportionality factor

$$\alpha = \frac{1}{\sigma_X^2}\int_{-\infty}^{\infty} V(x)(x - \langle X\rangle)p_X(x)dx. \tag{37}$$

Because

$$\langle V(x)\rangle = \int_{-\infty}^{\infty} V(x)\frac{1}{\sqrt{2\pi\sigma_X^2}}\exp\left[-\frac{(x-\langle X\rangle)^2}{2\sigma_X^2}\right]dx$$

we can rewrite Eq. (37) by

$$\alpha = \frac{d}{d\langle X\rangle}\langle V(X)\rangle\Big|_{\sigma_X=\text{const}}. \tag{38}$$

If we apply this theorem to the Gaussian process $A(t)$ and to the transformation $V(A) = \theta(A - \gamma + 1/(2N)) = Y_\gamma$ we obtain the following relation for the cross-correlation between the synchronous output and the common stimulus:

$$C_{Y_\gamma,s} = \alpha_G C_{A,s} = \alpha_G C_{b,s}. \tag{39}$$

The last equality holds true because all box trains are statistically equivalent, such that $\langle A(0)s(\tau)\rangle = \langle N^{-1}\sum_{k=1}^{N} b_k(0)s(\tau)\rangle = \langle b(0)s(\tau)\rangle$. According to Eq. (38) the proportionality factor is obtained by taking the derivative of Eq. (30) with respect to the mean activity R_0:

$$\begin{aligned}\alpha_G &= \frac{d}{dR_0}\langle Y_\gamma\rangle^G\Big|_{\sigma_A=\text{const}} = p_A^G\left(\gamma - \frac{1}{2N}\right)\\ &= \frac{1}{\sqrt{2\pi\sigma_A^2}}\exp\left[-\frac{\beta_\gamma^2}{2}\right].\end{aligned} \tag{40}$$

In the last line we have expressed the dependence on γ by the important parameter

$$\beta_\gamma = \frac{\gamma - R_0 - 1/(2N)}{\sigma_A}. \tag{41}$$

Thus, the proportionality factor α_G is a Gaussian function in γ, centered around $R_0 + 1/2N$. For a large population we obtain

$$\lim_{N\to\infty}\alpha_G(\gamma) = \frac{1}{\sqrt{2\pi\langle s_e^2\rangle}}\exp\left[\frac{-(\gamma - R_0)^2}{2\langle s_e^2\rangle}\right]. \tag{42}$$

Turning now to the Fourier domain, by virtue of Eqs. (10) and (39), the cross-spectrum between the partial synchronous output and the common stimulus has the same frequency dependence as the cross-spectrum between the single box train with the stimulus

$$S_{s,Y_\gamma}(f) = \alpha_G(\gamma)S_{s,b}(f). \tag{43}$$

By the linear response ansatz, Eq. (14), and because $\langle s\rangle = 0$

$$C_{bs}(\tau) = \langle R(0)s(\tau)\rangle_s = \langle s_e(0)s(\tau)\rangle, \tag{44}$$

such that

$$S_{s,b}(f) = \tilde{B}\chi S_s(f). \tag{45}$$

The absolute value of the single box-train cross-spectrum is therefore given by [using Eq. (20)]

$$|S_{s,b}(f)| = \Delta\text{sinc}(\Delta\pi f)|\chi(f)|S_s(f). \tag{46}$$

For the cross-spectrum between the synchronous output and the common stimulus we obtain in the Gaussian approximation

$$\left|S_{s,Y_\gamma}(f)\right| = \frac{e^{-\beta_\gamma^2/2}}{\sqrt{2\pi\sigma_A^2}}\Delta\text{sinc}(\Delta\pi f)|\chi(f)|S_s(f). \tag{47}$$

B. Combinatorial approach

One can directly compute the cross-spectrum of the synchronous output using the combinatorial product representation, Eq. (7). This ansatz leads, like the Gaussian approach, to a cross-spectrum which is proportional to the single box train cross-spectrum $S_{s,b}(f)$. For the proportionality factor we derive in the combinatorial approach

$$\alpha_C = \sum_{j=\gamma N}^{N} a_j\binom{N}{j}jR_0^{j-1}\left(1 + \frac{(j-1)(j-2)}{2}\frac{\langle s_e^2\rangle}{R_0^2}\right). \tag{48}$$

The derivation of Eq. (48) is shown in Appendix C.

At the first glance surprising, using Eq. (48) in combination with Eq. (35) yields

$$\alpha_C = \frac{d}{dR_0}\langle Y_\gamma\rangle_C, \tag{49}$$

i.e., the general relation Eq. (38) holds true in this approximation as well.

Figure 6 shows the absolute value of the cross-spectrum of the synchronous output for a population of ten simulated LIF neurons, normalized to its maximum for different synchrony thresholds γ (colored solid lines). One sees that these rescaled spectra almost overlap, i.e., they share approximately the same frequency dependence, which is well described by the

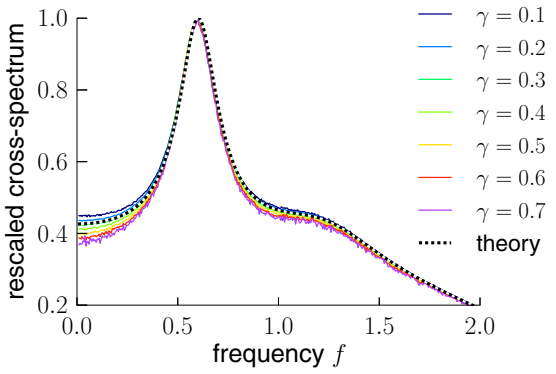

FIG. 6. Cross-spectrum between partial synchronous output and common noise is proportional to the one of the single box train. Absolute value of the cross-spectrum, $|S_{s,Y_\gamma}(f)|$, rescaled by its maximal value for various synchrony thresholds γ. Simulation results (colored solid lines) are compared to the theoretical prediction, Eq. (47), normalized by the maximum (black dashed line). Parameters: $\mu = 1.2, D = 0.01, c = 0.1, R_0 = 0.2, N = 10$.

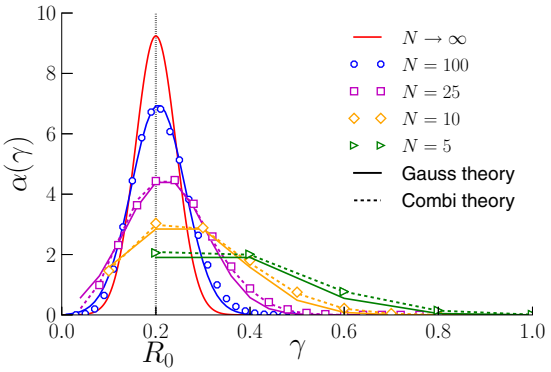

FIG. 7. Absolute value of the cross-spectrum is maximal if the synchrony threshold is set to the mean population activity. The proportionality constant α quantifies how much larger the cross-spectrum between the partial synchronous output and the stimulus is, in comparison to the single-neuron response [$S_{s,Y_\gamma}(f) = \alpha(\gamma) S_{s,b_k}(f)$]. α is plotted over the synchrony threshold γ for various population sizes N as indicated. In the simulations (symbols) $\alpha(\gamma)$ was taken as the ratio of the maxima of $S_{Y_\gamma,s}$ and S_{s,b_k}. The simulation results are compared to the combinatorial approximation, Eq. (48), (dashed lines) and the Gaussian theory, Eq. (40), (solid lines). The red solid line marks the limit case for infinite large populations, given by Eq. (42). The vertical line marks the mean activity value R_0. Parameters: $\mu = 1.2, D = 0.01, c = 0.1, R_0 = 0.2$.

single box train cross-spectrum $|S_{s,b}(f)|$ given by Eq. (46) (black dashed line). One observes slight deviations for small frequencies, which are not captured by the linear response approach.

In Fig. 7 we plot both approximations of the proportionality factor $\alpha(\gamma)$ for different population sizes. The combinatorial approach, Eq. (48), (dashed lines) is in excellent agreement with the simulation results. The Gaussian approximation, Eq. (40), (solid lines) slightly underestimates α for small population sizes, but gives very good results for larger populations (see $N = 100$) where we cannot evaluate Eq. (48) numerically any more.

VI. POWER SPECTRUM OF THE PARTIAL SYNCHRONOUS OUTPUT

The common noise does not only affect the cross-correlation but also the autocorrelation of the synchronous activity. However, even if no common stimulus is present, the calculation of the power spectrum of Y_γ is a non-trivial problem. For approximations of the power spectrum, $S_{Y_\gamma}(f)$, we will again employ the two different approaches.

A. Gaussian approach

For any stationary Gaussian process X and any smooth transformation $V(X) = Y$, the autocovariance $C_{YY}(\tau) = \langle Y(0)Y(\tau)\rangle - \langle Y\rangle^2$ of process Y can be expressed by the autocovariance of X [28]:

$$C_{YY}(\tau) = \sum_{n=1}^{\infty} \frac{1}{n!} \left\langle \frac{d^n}{dX^n} V(X) \right\rangle^2 C_{XX}^n(\tau). \tag{50}$$

If we assume the activity A to be Gaussian distributed, we can apply Eq. (50) to get an expression of the autocovariance of the partial synchronous output

$$C_{Y_\gamma Y_\gamma}(\tau) = \sum_{n=1}^{\infty} \frac{1}{n!} \left\langle \frac{d^n}{dA^n} \theta\left(A - \gamma + \frac{1}{2N}\right) \right\rangle^2 C_{AA}^n(\tau) \tag{51}$$

Although the Heaviside function is not a smooth function, we can formally differentiate it, which leads to a δ-distribution and its derivatives. Equation (51) considers only averages of these derivatives. These are integrals over the probability distribution p_A^G and hence, it is clear how this δ-function and further derivatives need to be evaluated. For $n \geqslant 1$ we obtain

$$\begin{aligned} &\left\langle \frac{d^n}{dA^n} \theta(A - \gamma) \right\rangle \\ &\quad = (-1)^{n-1} \int_0^1 \delta\left(A - \gamma + \frac{1}{2N}\right) \frac{d^{n-1} p_A^G(A)}{dA^{n-1}} dA \\ &\quad = (-1)^{n-1} \frac{d^{n-1}}{dA^{n-1}} p_A^G(A) \Big|_{A=\gamma-\frac{1}{2N}}. \end{aligned} \tag{52}$$

The nth derivative of the normal distribution can be expressed in terms of Hermite polynomials (probabilistic version), $He_n(x) := (-1)^n e^{x^2/2} \frac{d^n}{dx^n} e^{-x^2/2}$, such that

$$\frac{d^n}{dA^n} p_A^G(A) \Big|_{A=\gamma-\frac{1}{2N}} = \frac{(-1)^n}{\sigma_A^n} He_n(\beta_\gamma) p_A^G\left(\gamma - \frac{1}{2N}\right), \tag{53}$$

where β_γ is given in Eq. (41).

Plugging Eqs. (52) and (53) into Eq. (51), we obtain

$$C_{Y_\gamma Y_\gamma}(\tau) = \frac{e^{-\beta_\gamma^2}}{2\pi\sigma_A^2} \sum_{n=0}^{\infty} \frac{He_n^2(\beta_\gamma)}{(n+1)!\sigma_A^{2n}} {C_{AA}}^{n+1}(\tau). \tag{54}$$

The Fourier transform of this autocorrelation function yields an expression for the power spectrum of the synchronous output

$$S_{Y_\gamma}(f) = \frac{e^{-\beta_\gamma^2}}{2\pi\sigma_A^2} \left[S_A(f) + \sum_{n=1}^{\infty} \frac{He_n^2(\beta_\gamma)}{(n+1)!} \frac{1}{\sigma_A^{2n}} \overset{n}{\ast} S_A(f) \right], \tag{55}$$

where S_A is given by Eq. (24). By '$\overset{n}{\ast} S$' we denote the n-fold convolution of the function S with itself ($\overset{1}{\ast} S = S * S$, $\overset{2}{\ast} S = S * S * S$,...). The power of the synchronous output can be thus expressed by a weighted sum of convolutions of the activity's power spectrum.

Although we now have all the ingredients to evaluate Eq. (55), it turns out that the numerical evaluation of the infinite sum of convolutions is difficult for most parameter regimes, i.e., the sum cannot be truncated without making a seizable error. However, we can derive an alternative expression [completely equivalent to Eq. (55)] for the power spectrum as follows.

The Hermite polynomials appearing in Eq. (54) satisfy the so-called Mehler's formula [29]:

$$\sum_{n=0}^{\infty} \frac{a^n}{n!} (He_n(x))^2 = \frac{1}{\sqrt{1-a^2}} \exp\left[-x^2 \frac{a^2 - a}{1 - a^2}\right]. \tag{56}$$

In order to apply this formula we rewrite the terms in Eq. (54):

$$\frac{He_n^2(\beta_\gamma)}{(n+1)!}\left(\frac{C_{AA}(\tau)}{\sigma_A^2}\right)^{n+1} = \int_0^{\rho_A(\tau)} da\,\frac{a^n}{n!}He_n^2(\beta_\gamma), \quad (57)$$

where

$$\rho_A(\tau) = \frac{C_{AA}(\tau)}{\sigma_A^2} = \frac{\mathrm{IFT}(S_A)}{\sigma_A^2} \quad (58)$$

is the normalized autocorrelation function of the population activity, which can be derived by taking the inverse Fourier transform (IFT) of Eq. (24). With Eq. (57), the infinite sum in Eq. (54) is replaced by an integral, resulting in the desired alternative expression for the autocovariance of the synchronous output

$$C_{Y_\gamma Y_\gamma}(\tau) = \frac{1}{2\pi}\int_0^{\rho_A(\tau)} da\,\frac{1}{\sqrt{1-a^2}}\exp\left[-\frac{\beta_\gamma^2}{1+a}\right], \quad (59)$$

and to the power spectrum

$$S_{Y_\gamma}(f) = \frac{1}{2\pi}\mathrm{FT}\left(\int_0^{\rho_A(\tau)} da\,\frac{1}{\sqrt{1-a^2}}\exp\left[-\frac{\beta_\gamma^2}{1+a}\right]\right), \quad (60)$$

where FT stands for the Fourier transform.

The evaluation of the expression Eq. (60) involves three integrals: two Fourier transforms and the integral over a. This is manageable compared to the large number of convolutions that potentially have to be evaluated in Eq. (55). Unfortunately, there is no closed analytical solution of the integral in Eq. (59) for a general value of γ. An exception is the case $\gamma = R_0$, i.e., when the synchrony threshold is set to the mean activity, leading to $\beta_\gamma \approx 0$. For this case we obtain

$$S_{Y_{R_0}}(f) \approx \frac{1}{2\pi}\mathrm{FT}[\arcsin(\rho_A)]. \quad (61)$$

In particular, if we assume that the correlation function contributes mainly for long times where $|\rho_A| \ll 1$ and $\arcsin(\rho_A) \approx \rho_A$, we can further approximate the power spectrum by

$$S_{Y_{R_0}}(f) \approx \frac{1}{2\pi}\frac{S_A}{\sigma_A^2}. \quad (62)$$

Equation (61) describes simulation results for $\gamma = R_0$ indeed very well (see Fig. 8), and even the simple approximation Eq. (62) gives a rough estimate. Hence, if the synchrony threshold is set to the mean activity, the power spectrum of the synchronous output is approximately proportional to the power spectrum of the population activity, i.e., to the power of all spikes.

B. Combinatorial product approach

The derivation of the power spectrum in the combinatorial product approach is much more cumbersome than the respective calculation in the Gaussian approach and delegated to Appendix D. The main result for the power spectrum of the synchronous output in case of independent spike trains ($c = 0$)

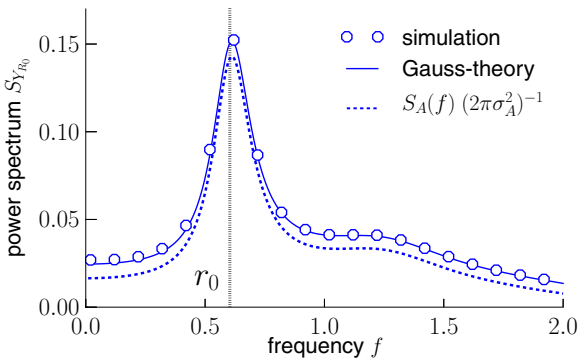

FIG. 8. For $\gamma = R_0$ the power spectrum of the synchronous output is approximately proportional to the power spectrum of the population activity. Power spectrum of the partial synchronous output if the synchrony threshold γ is set to the mean activity R_0. Simulation results (circles) are compared to the Gaussian approximation Eq. (61) (solid line) and to Eq. (62) (dashed line). The spectra have their maximum at roughly the single neuron firing rate $r_0 = 0.58$ (vertical dotted line). Parameters: μ=1.2, D=0.01, c=0.1, $R_0 = 0.2$, $N = 100$.

reads

$$S_{Y_\gamma} = \sum_{j,j'=\gamma N}^{N} a_j a_{j'} R_0^{j+j'} \sum_{m=\max(1,j+j'-N)}^{\min(j,j')} \frac{\#_{j,j',m}}{R_0^{2m}} \underset{m-1}{*} \hat{S}_b \quad (63)$$

with $\hat{S}_b(f) = S_b(f) + R_0^2\delta(f)$ and

$$\#_{j,k,m} = \binom{N}{m}\binom{N-m}{j-m}\binom{N-j}{k-m}. \quad (64)$$

We only present the spectrum in zeroth order of the common stimulus power because this result already gives a reasonable approximation of the frequency dependence of $S_{Y_\gamma}(f)$ for weak stimuli. For completeness, we also state the result in first order of the common stimulus' variance in Eq. (D7) in the Appendix.

C. Discussion of the power spectrum

Equation (60) illustrates that within the Gaussian approach the power spectrum depends on the synchrony threshold γ only through the key parameter β_γ^2. The parameter β_γ, Eq. (41), is essentially the distance between γ and the mean activity R_0, normalized by the activities standard deviation. Note that for any $\gamma \leqslant R_0$ there is always a $\gamma' > R_0$, namely $\gamma' = 2R_0 + 1/N - \gamma$, such that $\beta_\gamma^2 = \beta_{\gamma'}^2$. Hence, the Gaussian theory predicts that the corresponding power spectra of Y_γ and $Y_{\gamma'}$ are equal.

In Fig. 9 we compare the Gaussian approximation, Eq. (60), to simulations of a population of 100 LIF neurons. The theory agrees well with the simulation results and illustrates that the overall synchrony power is maximal for $\gamma = R_0$ ($\beta_\gamma \approx 0$) and the magnitude of power spectra drops as β_γ^2 increases. As predicted by theory, the power spectra corresponding to γ-values with the same β_γ^2-value are very close to each other, especially for larger frequencies. At low frequencies, the power spectrum for $\gamma < R_0$ is larger than for $\gamma' > R_0$, if $\beta_\gamma^2 = \beta_{\gamma'}^2$ (see inset in Fig. 9).

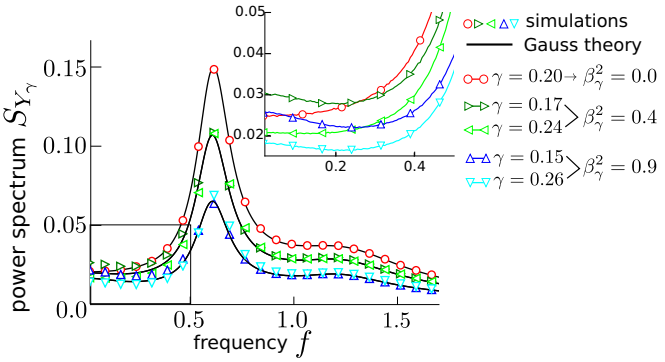

FIG. 9. The distance of the synchrony threshold γ to the mean activity determines the magnitude of the power of the synchronous output. Power spectrum of the partial synchronous output for a population of $N = 100$ LIF neurons for various synchrony thresholds γ. The Gaussian theory Eq. (60) predicts the identical result for γ-values which lead to the same value of $\beta_\gamma^2 = (\gamma - R_0 - 1/(2N))^2/\sigma_A^2$. The inset shows the power spectrum for small frequencies. Parameters: $\mu = 1.2, D = 0.01, c = 0.1, R_0 = 0.2, N = 100$.

In Fig. 10 we compare both theories with simulation results for an LIF population of only ten neurons. As expected for small populations, the Gaussian theory (black solid lines) does not work as well as for $N = 100$, but still gives a reasonable approximation. The main limitation of the Gaussian approach is that it does not distinguish between γ-values which lead to the same value of β_γ^2 but yield different spectra in the simulations, cf. data for $\gamma = 0.1$ (blue triangle right) and $\gamma = 0.4$ (green diamond). The combinatorial approach, Eq. (63), (dashed lines) gives a different result for every γ value and approximates the simulation results better. Because we neglect in Eq. (63) the influence of the weak common stimulus, this approximation underestimates the magnitude of the power spectrum of the synchronous output. We have verified that Eq. (63) describes perfectly well simulation results of the power spectrum for $c = 0$ (not shown).

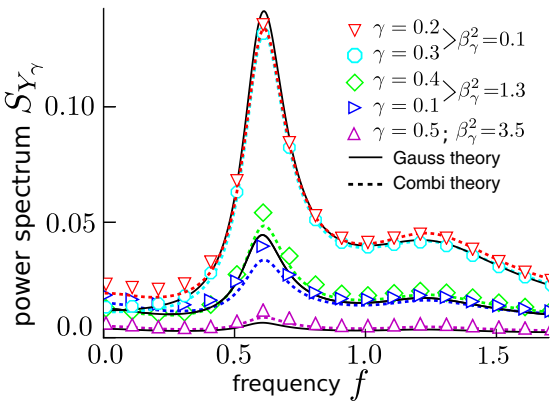

FIG. 10. For small populations, the combinatorial approach works better than the Gaussian one. Power spectrum of the partial synchronous output for a small population of ten LIF-neurons for various synchrony-thresholds γ as indicated. Simulation results (symbols) are compared to the Gaussian approximation Eq. (60) (black solid lines) and the combinatorial approximation (dashed lines) Eq. (63). Parameters: $\mu = 1.2, D = 0.01, c = 0.1, R_0 = 0.2, N = 10$.

What happens as $\gamma \to 1$, i.e., when the synchronous output is non-zero only if all neurons fire simultaneously? In this case the distance parameter β_γ^2 is large, such that the integrand in Eq. (59) is very small, i.e.,

$$\frac{1}{\sqrt{1-a^2}} \exp\left[-\frac{\beta_{\gamma\to 1}^2}{1+a} \right] \ll 1 \tag{65}$$

unless a is close to one, which only occurs if $\rho_A(\tau) \approx 1$. As a consequence, the correlation function is strongly peaked around $\tau = 0$, leading in the Fourier domain to a flat power spectrum

$$S_{Y_{\gamma\to 1}}(f) \approx \text{const.} \tag{66}$$

This behavior is not surprising. If γ is close to one, synchronous events become very rare and statistically independent of each other, i.e., we deal with a rare-event statistics which is Poissonian (flat power spectrum). The argument involving Eq. (65) also holds true in a large population for $\gamma \to 0$ because β_γ^2 attains high values in this case as well. The variability of the synchronous output is then determined by the rare events of (almost) complete silence in the population.

The limits of extreme γ values are explored in Fig. 11. In panel (a) the logarithmic scale for the spectra illustrates the strong reduction in their magnitude for both, $\gamma \to 1$ and

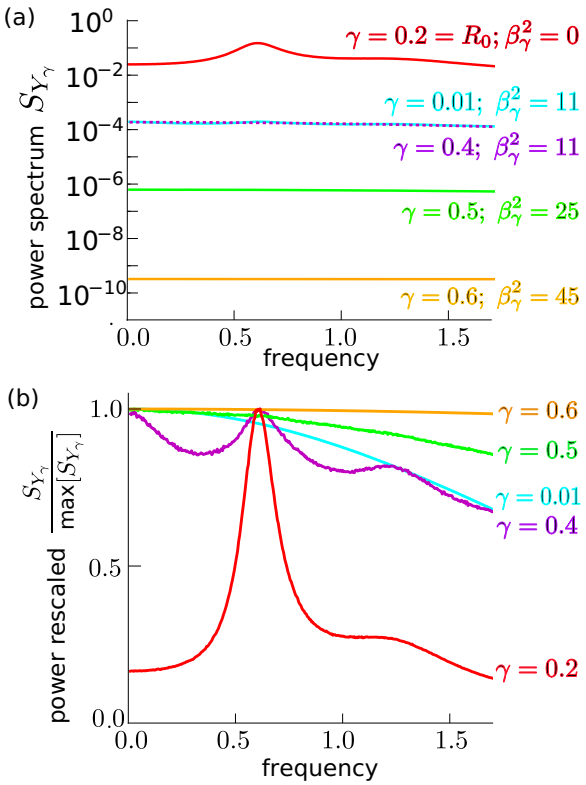

FIG. 11. The power spectrum of the synchronous output converges to a constant as $\gamma \to 1$ or $\gamma \to 0$. Power spectrum of the partial synchronous output for various synchrony threshold values γ. (a) Total value in log-scale. (b) S_{Y_γ} scaled by its maximal value. The power spectrum is maximal and the most peaked for $\gamma = R_0$ (red line). As γ approaches one or zero, the power spectrum converges to a flat spectrum as predicted by Eq. (66). Parameters: $\mu = 1.2, D = 0.01, c = 0.1, R_0 = 0.2, N = 100$.

$\gamma \to 0$. The flattening of the spectra in these limits is better seen on a linear scale [Fig. 11(b)], in particular if the spectra are rescaled by their maximal value. The power spectrum becomes indeed constant as γ approaches one and is already rather flat for $\gamma \geqslant 0.6$ in the shown frequency range. The flattening effect for $\gamma \to 0$ (see $\gamma = 0.01$) is less pronounced, because $\beta^2_{\gamma=0} \ll \beta^2_{\gamma=1}$.

VII. APPLICATION TO NON-WHITE COMMON STIMULI

So far, in all simulations, we considered the common noise to be white, which is useful in order to see how the system reacts to an arbitrary frequency component of a common input. However, white noise is certainly not a very natural stimulus. We can in principle employ our results to a Gaussian stimulus of arbitrary temporal correlation as long as it is weak. For instance, we can consider the Ornstein-Uhlenbeck process (OUP)

$$\tau_s \dot{s} = -s + \sqrt{2Dc}\xi_s(t), \tag{67}$$

where ξ_s is Gaussian white noise. The intensity of s (integral over its autocorrelation function) is again Dc, but now it has a positive autocorrelation time τ_s. The power spectrum of process Eq. (67) reads

$$S(f) = \frac{2Dc}{1 + (2\pi f \tau_s)^2}. \tag{68}$$

Figure 12 shows the cross- and power spectrum of the synchronous output with synchrony threshold $\gamma = 0.25$ of an LIF population driven by a common OUP for two different autocorrelation times. The power spectrum of the corresponding stimulus is shown in the inset in Fig. 12(a). We see that the theory agrees well with simulation results, also in the case of colored input.

For small autocorrelation times τ_s (see purple circles in Fig. 12) we see a similar behavior to the white noise case. For larger values of τ_s (see triangles in Fig. 12) the power of the stimulus (and of the effective stimulus) is diminished already at moderate frequencies, such that the cross-spectrum between the synchronous output and the stimulus is concentrated at low frequencies. As a consequence, the ratio between the power of the synchronous output at low and high frequencies increases with τ_s [see Fig. 12(b)]. Because we fix the noise intensity, an increase in the autocorrelation time τ_s leads to a decrease in the variance of the stimulus, such that the mean magnitude of the power of the synchronous output is decreased as well.

VIII. SUMMARY

In this paper we have studied the statistics of the partial synchronous output of a neuronal population which is driven by a weak common noise. This synchronous output can be regarded as a simple model of a postsynaptic coincidence detector which is only activated if at least a fixed fraction γ of the presynaptic population fires simultaneously. Here, we derived analytical approximations for the statistics of the partial synchronous output: for its mean value, power spectrum, and its cross-spectrum with the stimulus. We investigated how these statistics depend on the activation threshold γ.

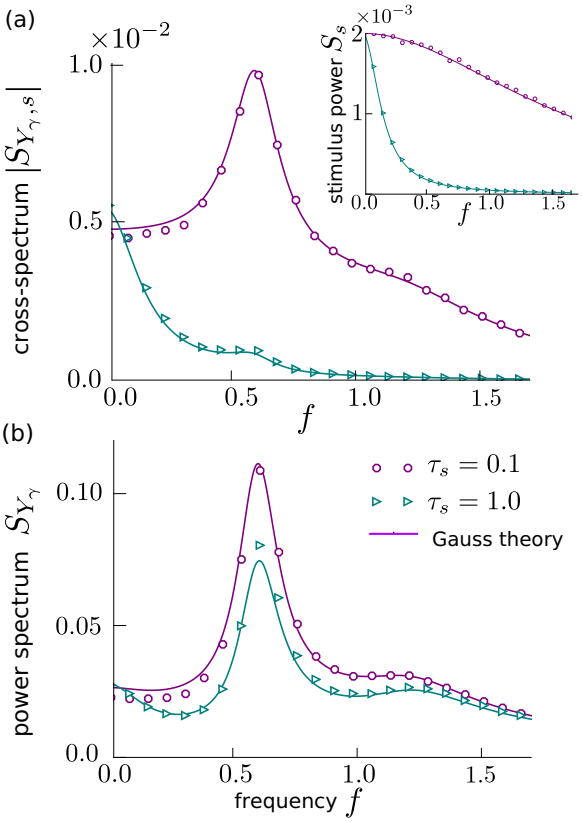

FIG. 12. Theory is also applicable to colored noise. Spectra of the partial synchronous output ($\gamma = 0.25$) for an LIF population which is driven by a common Ornstein-Uhlenbeck process, given by Eq. (67), with two different autocorrelation times τ_s as indicated. (a) Cross-spectrum between synchronous output and the common stimulus. The inset shows the power spectrum of the OUP. (b) Power spectrum of the synchronous output. Symbols mark simulation results and the solid lines show the theoretic predictions (47), (68), and (60). Remaining parameters: $\mu = 1.2, D = 0.01, c = 0.1, R_0 = 0.2, N = 100$.

For the analytical approximations we employed two different approaches. In the Gaussian approach the synchronous output is a threshold function of the summed population activity $A(t)$ and the activity is assumed to have a Gaussian distribution. Under this assumption, all statistics of the synchronous output can be expressed in terms of the statistics of the population activity. The Gaussian approach results in reasonable, sometimes even excellent approximations of the investigated statistics, especially for large populations. The advantage of the Gaussian approach is the simplicity of the formulas, making the role of γ more transparent. For instance, it predicts a particular symmetry in the dependence of power and cross-spectra on γ. The statistics is indistinguishable if the synchrony threshold has the same distance to the mean activity R_0, i.e., for values of γ that lead to the same value of $|\beta_\gamma| = |\gamma - R_0 - 1/(2N)|/\sigma_A$. In numerical simulations this symmetry is found to be valid to a good approximation. It reflects the similarity of joint firing and joint silence of neurons in the population.

In the combinatorial approach, the synchronous output is expressed by products of the box-filtered spike trains. This yields generally more accurate results. In contrast to the

Gaussian approach it differentiates between γ-values that lead to the same value of $|\beta_\gamma|$ and can quantitatively describe the small differences between these cases. However, the resulting equations are quite cumbersome and do not provide much insight about the roles of parameters. In addition, in practice they can be evaluated only for small populations because of the required numerical effort to compute the combinatorial factors occurring in the formulas.

We showed that for all values of γ and for any population size, the cross-spectrum of the synchronous output with the common stimulus is approximately proportional to the cross-spectrum between the single neuron and the stimulus. This result is in line with Ref. [22], where the authors showed this proportionality for small populations for the case $\gamma = 1$. It also implies that the cross-spectrum between synchronous output and stimulus displays the same frequency dependence as the cross-spectrum of the population activity with the stimulus. In conclusion, the temporal correlations between the synchronous events and the stimulus are similar to those between the single or summed spike trains and the stimulus. This is somewhat surprising because the synchronous output is a strongly non-linear function of the population activity. Apart from the frequency dependence, the amplitude of the cross-spectrum is mainly determined by the aforementioned distance $|\beta_\gamma|$ of the threshold γ to the mean activity, and decays exponentially ($\sim e^{-\beta_\gamma^2}$).

The most demanding challenge in our study was the approximation of the power spectrum of the synchronous output. For this spectrum the synchrony threshold does not only influence the magnitude (which again decreases with $|\beta_\gamma|$), but also the frequency dependence. We showed that for $\gamma = R_0$ the power spectrum is approximately proportional to the power spectrum of the population activity. This is due to the fact that in this case the synchronous output is a symmetric two-state version of the population activity. In the opposite limits, as γ goes to one or zero, the power spectrum approaches a flat function, revealing the Poisson-like character of synchronous events if the synchrony threshold is set far away from the mean activity.

Summarizing, the amplitude of the synchronous output's spectra is most drastically reduced if the synchrony threshold differs strongly from R_0 (i.e., for $|\beta_\gamma| \gg 1$). With respect to temporal aspects, the synchronous output differs mainly in its autocorrelation statistics from those of the population activity and again these differences are most pronounced for $|\beta_\gamma| \gg 1$. As we pointed out in the introduction, it is simple to extract the synchronous output of a homogeneous population from repeated trials of frozen-noise stimulation in experiment. Hence, it should not be too complicated to test our theoretical predictions with real experimental data.

What are the consequences for the postsynaptic cell that we wanted to mimic with Y_γ? The postsynaptic cell sets the value of R_0 by the time it integrates incoming input. It also determines the synchrony threshold γ by its firing threshold. For $\gamma = R_0$ the synchronous output is most sensitive to changes in the common stimulus. However, in this case, it does not properly reflect true synchronization events but rather represents a binary version of the summed population activity. In order for the postsynaptic cell to measure synchronization that is beyond average, and therefore to encode different information than the summed activity does, the synchrony threshold should not be too close to the mean activity. Beyond average synchronization is measured if $\gamma > R_0 + \sigma_A$ (joint firing) or if $\gamma < R_0 - \sigma_A$ (joint silence). Furthermore, for large values of N, a real postsynaptic neuron is not likely to operate in the extreme regime where γ is close to zero or one. We have seen that for these limit values, the synchronous output resembles a rare-event pulse train and is not variable enough to encode any information about an incoming weak stimulus.

It is an interesting question how exactly the information transmission of the synchronous output is influenced by the choice of γ. Does the synchronous output preferentially encode certain frequency bands of the stimulus as shown for $\gamma = 1$ and small N in Refs. [14] and [22]? The question of information filtering can be approached by computing the coherence function between the synchronous output and the common stimulus (for some limitations of this approach, see [30]), for which we have derived all necessary quantities in this paper. Thus, our results will be useful in future studies to explore how the readout mechanism of a postsynaptic cell influences its information selection.

In this paper we exclusively study a neuronal population, where the neurons do not influence each other. It would be worthwhile to extend our theory to recurrently coupled networks. These can reveal a broad diversity of synchrony states [31,32] and it is a deeply interesting question how the network state impacts signal transmission of the synchronous activity.

ACKNOWLEDGMENTS

We would like to acknowledge funding by DFG (Sachbeihilfe LI 1046/2-1) and BMBF 284 (FKZ: 01GQ1001A).

APPENDIX A: SPECIFIC EQUATIONS FOR THE LIF-MODEL

To implement our theory to the special case of the stochastic leaky integrate-and-fire neuron model with the voltage dynamics

$$\dot{v} = -v + \mu + \sqrt{2D}\xi(t) \tag{A1}$$

with $\langle \xi(t)\xi(t')\rangle = \delta(t-t')$, zero reset value and threshold one, the following expressions are necessary.

The mean firing rate is given by [33]

$$r_0 = \left[\sqrt{\pi}\int_{(\mu-1)/\sqrt{2D}}^{\mu/\sqrt{2D}} e^{y^2}\,\mathrm{erfc}(y)dy\right]^{-1}. \tag{A2}$$

The susceptibility of the firing rate can be expressed in terms of parabolic cylinder functions $\mathcal{D}_\alpha(z)$ [34,35]

$$\chi(f) = \frac{r_0 2\pi i f}{\sqrt{D}(2\pi i f - 1)} \frac{\mathcal{D}_{2\pi i f-1}\left(\frac{\mu-1}{\sqrt{D}}\right) - e^{\epsilon}\mathcal{D}_{2\pi i f-1}\left(\frac{\mu}{\sqrt{D}}\right)}{\mathcal{D}_{2\pi i f}\left(\frac{\mu-1}{\sqrt{D}}\right) - e^{\epsilon}\mathcal{D}_{2\pi i f}\left(\frac{\mu}{\sqrt{D}}\right)}, \tag{A3}$$

where $\epsilon = (2\mu - 1)/(4D)$. The power spectrum (without DC peak) of the spike train reads [36]

$$S_x(f) = r_0 \frac{\left|\mathcal{D}_{2\pi i f}\left(\frac{\mu-1}{\sqrt{D}}\right)\right|^2 - e^{2\epsilon}\left|\mathcal{D}_{2\pi i f}\left(\frac{\mu}{\sqrt{D}}\right)\right|^2}{\left|\mathcal{D}_{2\pi i f}\left(\frac{\mu-1}{\sqrt{D}}\right) - e^{\epsilon}\mathcal{D}_{2\pi i f}\left(\frac{\mu}{\sqrt{D}}\right)\right|^2}. \tag{A4}$$

APPENDIX B: COMBINATORIAL PRODUCT DEFINITION OF THE PARTIAL SYNCHRONOUS OUTPUT

The prefactors a_j of the combinatorial definition of the partial synchronous output, Eq. (7), can be derived in the following way. Let κ_j be the sum over all combinations of products of j box trains

$$\kappa_j(t) := \sum_{\substack{\text{over all}\binom{N}{j}\\ \text{combinations}\,\pi}} \prod_{k=1}^{j} b_{\pi_k}(t). \tag{B1}$$

Let n be the actual number of simultaneously spiking neurons at time t, i.e., $n = N \cdot A(t)$. Then $\kappa_j(t) = \binom{n}{j}$, if $n \geqslant j$ and it is zero otherwise.

The synchronous output can be described by

$$Y_\gamma(t) = \sum_{j=\gamma N}^{N} a_j \cdot \kappa_j(t), \tag{B2}$$

where we still have to determine the prefactors a_j. If $n < \gamma N$, then $Y_\gamma(t) = 0$ (as it should be) because $\kappa_j(t) = 0$ for $n < j$ by definition. If $n \geqslant \gamma N$ terms with $j > n$ do not contribute to the sum and we obtain

$$Y_\gamma(t) = \sum_{j=\gamma N}^{n} a_j \binom{n}{j}. \tag{B3}$$

In order for $Y_\gamma(t)$ to have the value one for any n with $N \geqslant n \geqslant \gamma N$, the following recursive formula must hold:

$$a_n = 1 - \sum_{j=\gamma N}^{n-1} a_j \binom{n}{j}, \tag{B4}$$

which can be translated to the explicit form

$$a_j = (-1)^{j-\gamma N} \binom{j-1}{j-\gamma N}. \tag{B5}$$

APPENDIX C: ANALYTICAL DERIVATION OF THE CROSS-SPECTRUM USING THE COMBINATORIAL PRODUCT DEFINITION

Using the combinatorial product definition of Y_γ, Eq. (7), the cross-covariance between the partial synchronous output and the common stimulus reads

$$\begin{aligned} C_{Y_\gamma,s}(\tau) &= \langle Y_\gamma(0)s(\tau)\rangle \\ &= \sum_{j=\gamma N}^{N} a_j \sum_{\substack{\text{over all}\binom{N}{j}\\ \text{combinations}\,\pi}} \left\langle \prod_{k=1}^{j} \langle b_{\pi_k}(0)\rangle_{\xi_{\pi_k}} s(\tau) \right\rangle_s \\ &= \sum_{j=\gamma N}^{N} a_j \binom{N}{j} \left\langle \langle b(0)\rangle_\xi^j s(\tau)\right\rangle_s, \end{aligned} \tag{C1}$$

where we used that the stimulus ($\langle s\rangle = 0$) is independent of the intrinsic noise and that all individual box trains, $b_k(t)$, are independent and identically distributed. Using the linear response ansatz Eq. (14), we further evaluate Eq. (C1) up to the second order of the variance of s:

$$\left\langle \langle b(0)\rangle_\xi^j s(\tau)\right\rangle_s = \langle (R_0 + s_e(0))^j s(\tau)\rangle_s \tag{C2}$$

$$= j R_0^{j-1} \langle s_e(0)s(\tau)\rangle_s + \binom{j}{3} R_0^{j-3} \left\langle s_e^3(0)s(\tau)\right\rangle_s, \tag{C3}$$

where we used again the binomial formula Eq. (34) and that the stimulus s and the effective stimulus s_e are both Gaussian processes with zero mean value, such that $\langle s_e^2(0)s(\tau)\rangle = 0$. For any Gaussian random variables X_1, X_2, X_3, X_4 with zero mean holds $\langle X_1X_2X_3X_4\rangle = \langle X_1X_2\rangle\langle X_3X_4\rangle + \langle X_1X_3\rangle\langle X_2X_4\rangle + \langle X_1X_4\rangle\langle X_2X_3\rangle$, such that $\langle s_e^3(0)s(\tau)\rangle_s = 3\langle s_e^2\rangle\langle s_e(0)s(\tau)\rangle_s$. The cross-covariance Eq. (C1) reads therefore

$$C_{Y_\gamma,s}(\tau) = \alpha C_{s_e,s}(\tau) \tag{C4}$$

with the proportionality factor

$$\alpha = \sum_{j=\gamma N}^{N} a_j \binom{N}{j} j R_0^{j-1} \left(1 + \frac{(j-1)(j-2)}{2} \frac{\langle s_e^2\rangle}{R_0^2}\right). \tag{C5}$$

Because of Eq. (14), $C_{s_e,s} = C_{b,s}$ and thus Eq. (C4) reads in the Fourier domain

$$S_{s,Y_\gamma}(f) = \alpha S_{s,b}(f). \tag{C6}$$

APPENDIX D: ANALYTICAL DERIVATION OF THE POWER SPECTRUM USING THE COMBINATORIAL PRODUCT DEFINITION OF Y_γ

Using the combinatorial definition, Eq. (7), the autocorrelation function of the partial synchronous output reads

$$\begin{aligned} \langle Y_\gamma(0)Y_\gamma(\tau)\rangle &= C_{Y_\gamma Y_\gamma}(\tau) + \langle Y_\gamma\rangle^2 \\ &= \sum_{j,j'=\gamma N}^{N} a_j a_{j'} \sum_{\substack{\text{over all}\binom{N}{j}\\ \text{combinations}\,\pi}} \sum_{\substack{\text{over all}\binom{N}{j'}\\ \text{combinations}\,\pi'}} \left\langle \mathcal{P}_{\pi,\pi'}^{j,j'}\right\rangle, \end{aligned} \tag{D1}$$

where

$$\mathcal{P}_{\pi,\pi'}^{j,j'} := \prod_{k=1}^{j} b_{\pi_k}(0) \prod_{k'=1}^{j'} b_{\pi'_k}(\tau). \tag{D2}$$

The mean value of $\mathcal{P}_{\pi,\pi'}^{j,j'}$ depends on the number of matching pairs, $b_k(0)b_k(\tau)$, i.e., when the same neuron index appears twice in Eq. (D2). If there are exactly m matching pairs we find

$$\left\langle \mathcal{P}_{\pi,\pi'}^{j,j'}\right\rangle = \left\langle \langle b(0)b(\tau)\rangle_\xi^m \langle b(0)\rangle_\xi^{j-m} \langle b(\tau)\rangle_\xi^{j'-m}\right\rangle_s. \tag{D3}$$

If we neglect the influence of the weak stimulus $s(t)$, Eq. (D3) reads

$$\left\langle \mathcal{P}_{\pi,\pi'}^{j,j'}\right\rangle = \left(C_{bb}(\tau) + R_0^2\right)^m R_0^{j+j'-2m}, \tag{D4}$$

where $C_{bb}(\tau) = \langle b(0)b(\tau)\rangle - \langle b(0)\rangle^2$ is the autocovariance of the single box-train. Hence, instead of summing over all

combinations π and π' in Eq. (D1), we only need to sum over the number of matching pairs m, resulting in

$$C_{Y_\gamma Y_\gamma}(\tau) + \langle Y_\gamma \rangle^2 = \sum_{j,j'=\gamma N}^{N} a_j a_{j'} R_0^{j+j'} \sum_{m=\max(0,j+j'-N)}^{\min(j,j')} \#_{j,j',m} \left(\frac{C_{b,b}(\tau) + R_0^2}{R_0^2} \right)^m, \tag{D5}$$

where $\#_{j,j',m} = \binom{N}{m}\binom{N-m}{j-m}\binom{N-j}{j'-m}$ is the number of combinations of having exactly m matching pairs given fixed values of j and j'. By the convolution theorem we obtain for the power spectrum of Y_γ ($f \neq 0$):

$$S^{(0)}_{Y_\gamma}(f) = \sum_{j,j'=\gamma N}^{N} a_j a_{j'} R_0^{j+j'} \sum_{m=\max(1,j+j'-N)}^{\min(j,j')} \frac{\#_{j,j',m}}{R_0^{2m}} \overset{*}{m-1} \hat{S}_b(f) \tag{D6}$$

with $\hat{S}_b(f) = S_b(f) + R_0^2 \delta(f)$ being the power spectrum of the single box train including the DC-peak. Taking into account the δ-function in $\hat{S}_b$ is important, because it affects the convolutions.

We only state the linear-response approximation for the power spectrum up to the first order of the variance of the common stimulus

$$S^{(1)}_{Y_\gamma}(f) = \sum_{j,j'=\gamma N}^{N} a_j a_{j'} R_0^{j+j'} \sum_{m=\max(1,j+j'-N)}^{\min(j,j')} \frac{\#_{j,j',m}}{R_0^{2m}} \omega_{j,j',m}(f), \tag{D7}$$

where

$$\begin{aligned} \omega_{j,j',m} = \Bigg\{ & \left(1 + \left[\binom{j'-m}{2} + \binom{j-m}{2}\right] \frac{\langle s_e^2 \rangle}{R_0^2}\right) \overset{*}{m-1} \hat{S}_b \\ & + R_0^{-2}(j'-m)(j-m) S_{s_e} * \overset{*}{m-1} \hat{S}_b \\ & + m[j+j'-2m] \langle s_e^2 \rangle \overset{*}{m-2} \hat{S}_b \\ & + m[j+j'-2m+1] S_{s_e} * \overset{*}{m-2} \hat{S}_b \\ & + R_0^2 m(m-1) \left[\langle s_e^2 \rangle \overset{*}{m-3} \hat{S}_b + S_{s_e} * \overset{*}{m-3} \hat{S}_b \right] \Bigg\}. \end{aligned}$$

[1] Y. Dan, J. M. Alonso, W. M. Usrey, and R. C. Reid, Nat. Neurosci. **1**, 501 (1998).
[2] M. Stopfer, S. Bhagavan, B. H. Smith, and G. Laurent, Nature **390**, 70 (1997).
[3] P. Knig, A. K. Engel, and W. Singer, Trends Neurosci. **19**, 130 (1996).
[4] E. R. Kandel, J. H. Schwartz, and T. M. Jessel, *Principles of Neural Science* (McGraw-Hill Companies, New York, 2000).
[5] R. I. Wilson, Annu. Rev. Neurosci. **36**, 217 (2013).
[6] C. G. Galizia, Eur. J. Neurosc. **39**, 1784 (2014).
[7] L. Maler, J. Comp. Neurol. **516**, 376 (2009).
[8] B. Doiron, M. J. Chacron, L. Maler, A. Longtin, and J. Bastian, Nature **421**, 539 (2003).
[9] M. J. Chacron, B. Doiron, L. Maler, A. Longtin, and J. Bastian, Nature **423**, 77 (2003).
[10] J. de la Rocha, B. Doiron, E. Shea-Brown, K. Josic, and A. Reyes, Nature **448**, 802 (2007).
[11] J. Grewe, A. Kruscha, B. Lindner, and J. Benda (unpublished).
[12] J. Benda, A. Longtin, and L. Maler, Neuron **52**, 347 (2006).
[13] R. F. Galán, N. Fourcaud-Trocme, G. B. Ermentrout, and N. N. Urban, J. Neurosci. **26**, 3646 (2006).
[14] J. W. Middleton, A. Longtin, J. Benda, and L. Maler, J. Neurophysiol. **101**, 1160 (2009).
[15] S. Amari, H. Nakahara, S. Wu, and Y. Sakai, Neural Comp. **15**, 127 (2003).
[16] B. Lindner, B. Doiron, and A. Longtin, Phys. Rev. E **72**, 061919 (2005).
[17] E. Shea-Brown, K. Josić, J. de la Rocha, and B. Doiron, Phys. Rev. Lett. **100**, 108102 (2008).
[18] S. Ostojic, N. Brunel, and V. Hakim, J. Neurosci. **29**, 10234 (2009).
[19] R. D. Vilela and B. Lindner, J. Theor. Biol. **257**, 90 (2009).
[20] D. A. Leen and E. Shea-Brown, J. Math. Neurosci. **5**, 1 (2015).
[21] A. Kruscha and B. Lindner, Phys. Rev. E **92**, 052817 (2015).
[22] N. Sharafi, J. Benda, and B. Lindner, J. Comp. Neurosci. **34**, 285 (2013).
[23] W. Gerstner, W. M. Kistler, R. Naud, and L. Paninski, *Neuronal Dynamics: From Single Neurons to Networks and Models of Cognition* (Cambridge University Press, Cambridge, 2014).
[24] B. W. Knight, J. Gen. Physiol. **59**, 734 (1972).
[25] N. Fourcaud and N. Brunel, Neural Comput. **14**, 2057 (2002).
[26] W. Gerstner and W. M. Kistler, *Spiking Neuron Models* (Cambridge University Press, Cambridge, 2002).
[27] J. Bussgang, Crosscorrelation functions of amplitude-distorted Gaussian signals, MITRes Lab Elec Technical Report, 1952, pp. 1–4.
[28] A. Malakhov, *Cumulant Analysis of Stochastic Non-Gaussian Processes and Their Transformations* (in Russian) (Sov. Radio, Moskva, 1952), pp. 255–257.
[29] G. Watson, J. London Math. Soc. **1**, 194 (1933).
[30] D. Bernardi and B. Lindner, J. Neurophysiol. **113**, 1342 (2015).
[31] N. Brunel, J. Comp. Neurosci. **8**, 183 (2000).
[32] S. Ostojic, Nat. Neurosci. **17**, 594 (2014).
[33] L. M. Ricciardi, *Diffusion Processes and Related Topics on Biology* (Springer-Verlag, Berlin, 1977).
[34] B. Lindner and L. Schimansky-Geier, Phys. Rev. Lett. **86**, 2934 (2001).
[35] N. Brunel, F. S. Chance, N. Fourcaud, and L. F. Abbott, Phys. Rev. Lett. **86**, 2186 (2001).
[36] B. Lindner, L. Schimansky-Geier, and A. Longtin, Phys. Rev. E. **66**, 031916 (2002).